Dalton Transactions

Accepted Manuscript

ROYAL SOCIETY OF CHEMISTRY

www.rsc.org/dalton

Journal Name

RSCPublishing

ARTICLE

Cobalt selenium oxohalides: Catalysts for Water Oxidation

sCite this: DOI: 10.1039/x0xx00000x

Received 00th January 2012,
Accepted 00th January 2012

DOI: 10.1039/x0xx00000x

www.rsc.org/

Faiz Rabbani[a,b], Henrik Svengren[a], Iwan Zimmermann[a], Shichao Hu[a], Tanja Laine[c], Wenming Hao[a], Björn Åkermark[c], Torbjörn Åkermark[c], Mats Johnsson[a]

Two new oxohalides $Co_4Se_3O_9Cl_2$ and $Co_3Se_4O_{10}Cl_2$ have been synthesized by solid state reactions. They crystallize in the orthorhombic space group *Pnma* and the monoclinic space group *C2/m* respectively. The crystal structure of the two compounds are made up of similar building blocks; $Co_4Se_3O_9Cl_2$ is made up of $[CoO_4Cl_2]$, $[CoO_5Cl]$ and $[SeO_3]$ polyhedra and $Co_3Se_4O_{10}Cl_2$ is made up of $[CoO_4Cl_2]$ and $[SeO_3]$ polyhedra. As several Co-containing compounds have proved to be good catalysts for water oxidation, the activity of the two new compounds were compared with the previously found oxohalide $Co_5Se_4O_{12}Cl_2$ in reference to CoO and $CoCl_2$. The one electron oxidant $Ru(bpy)_3^{3+}$ was used as oxidizing species in a phosphate buffer and it was found that the activities of the oxohalide species were in between CoO and $CoCl_2$. The roles of Cl^- and PO_4^{3-} ions are discussed.

Introduction

In this study we have further investigated the system Co^{2+}-Se^{4+}-O-Cl and found two new compounds; (**1**) $Co_4Se_3O_9Cl_2$ and (**2**) $Co_3Se_4O_{10}Cl_2$. The building blocks of those compounds are alternating cobalt-oxo-chloride octahedra connected by Se-O bridges in a very similar fashion as in the previously known compound (**3**) $Co_5Se_4O_{12}Cl_2$ [1]. Transition metals tend to bond to both oxide- and halide ions in transition metal oxohalides while stereochemically active lone-pair cations such as Te^{4+} or Se^{4+} preferably form bonds only to oxygen due to differences in Lewis acidity. This chemical difference and the fact that both the halide ions and the one-sided coordination of the lone-pair cation Se^{4+} act as "chemical scissors" often results in formation of open crystal structures and low-dimensional arrangements of the transition metal ions [2-3].

A major obstacle in developing devices capable of converting solar energy into fuel, such as hydrogen, is capturing electrons from water. In the process, water is oxidizing to molecular O_2(g) to use these electrons to reduce protons to hydrogen. A number of efficient homogenous water oxidation catalysts (WOCs) based on the noble metals ruthenium and iridium has been developed during the last decade. However, the full utilization of solar energy probably requires the use of catalysts based on cheaper metals. Although simple cobalt salts were shown to catalyze water oxidation already in the 1980s [4-7] little progress has been made in the field until Kanan and Nocera recently showed that efficient WOCs could be generated electrochemically from cobalt ions and phosphate [7]. Since Co-containing phases have proved to be promising catalysts we decided to test our oxohalide compounds as water oxidation catalysts using $Ru^{3+}(bpy)_3(PF_6)_3$ as oxidant.

Experimental

Blue single crystals of **(1)** $Co_4(SeO_3)_3Cl_2$ and purple single crystals of **(2)** $Co_3Se_4O_{10}Cl_2$ were synthesized via solid state reactions in different experiments. The starting materials were; CoO (ABCR GmbH 97.999%), SeO_2 (Alfa Aesar 99.4%) and $CoCl_2$ (Sigma-Aldrich 97.0%). For **(1)** the non-stoichiometric mixture was 0.196 g (2.6 mmol) CoO; 0.113 g (0.87 mmol) $CoCl_2$ and 0.289 g (2.6 mmol) SeO_2 and for **(2)** the stoichiometric mixture was 0.075 g (1 mmol) CoO, 0.065 g (0.5mmol) $CoCl_2$, and 0.222 g (2 mmol) SeO_2. The powders were introduced into silica tubes (length = 5 cm, ∅ = 5.5 mm) which were dried for 2 h at 100°C and then evacuated, sealed and heated to 550°C and kept there for 96 hours in a muffle furnace. Purple single crystals of $Co_5(SeO_3)_4Cl_2$ **(3)** were synthesised from a stoichiometric mixture of the same starting materials [1].

Single crystal X-ray diffraction experiments were carried out on an Oxford Diffraction Xcalibur3 diffractometer equipped with a graphite monochromator. The data collection was performed using MoK_α radiation, $\lambda = 0.71073$ Å. Absorption correction and data reduction were done with the software CrysAlis RED [8]. The structure solution was performed with SHELXS-97 and the refinement with SHELXL-97 [9]. All atomic positions were refined anisotropically. Crystal data are reported in Supplementary material. Atomic coordinates and isotropic temperature parameters for all atoms are given in the supplementary material. The structural drawings are made with the program DIAMOND [10]. Bond valence sum calculations are performed according to Brown and Altermatt [11].

Nitrogen adsorption isotherms were measured at 77 K using a Micromeritics ASAP 2020 device. Before conducting the adsorption experiments, samples were degassed under

conditions of dynamic vacuum at a temperature of 150 ºC for 1 h. Specific surface areas (S_{BET}) were calculated using standard expressions for Brunauer–Emmet–Teller (BET) isotherms. For BET analyses, uptake of nitrogen at relative pressures of p/p_0 = 0.06 - 0.29 were used. The total pore volume (V_t) was estimated from the uptake at a p/p_0 = 0.99.

The evolution of oxygen was measured by mass spectrometry, details of the MS-system used for studies of oxidation/reduction of water have been described previously [12-13]. As oxidant $Ru^{3+}(bpy)_3(PF_6)_3$ at 1.26 *vs.* NHE [14], was used. Commonly, an experiment was carried out in a closed atmosphere reaction chamber system as follows: a catalyst was placed in the reaction chamber (16x150mm standard glass test tube) with a magnet stirrer and 0.75 ml 0.1M phosphate buffer solution of pH 6.0. The $Ru^{3+}(bpy)_3(PF_6)_3$ oxidant was subsequently loaded in a cut Eppendorf® tube which was held above the catalyst and the buffer solution inside the reaction chamber by a magnet controlled holder. The system was sealed to prevent leakage from atmospheric oxygen and evacuated with a roughing pump until the equilibrium pressure of H_2O(g), that is approximately 15 mbar at 13 °C and the oxygen pressure below the level for the studied reaction were reached. The reaction chamber was then introduced with ~5 mbar of the reference gas He, followed by pressure adjustment to fit the detection span making the system ready for the reaction to be studied in situ. The oxygen evolving reaction started by using external magnets to drop the beaker containing the oxidant into the buffer solution containing the catalyst, where the beaker was quickly emptied under maximum stirring. Both the evacuation and the reaction were performed under isothermal conditions. In the experiment with ^{18}O labeled water a semi-closed system was used and the buffer solution was instead prepared to contain 15% $H_2{}^{18}O$ and injected with a syringe trough a rubber membrane to the dry catalyst of ~1.9 µmol and oxidant of ~5.6 µmol to start the reaction. In experimental series designed for comparison the ratios of catalyst and oxidant have been kept at constant molar ratios. The exact amounts of chemicals used in the different experiments are presented in the supplementary materials. Turnover number (TN) is calculated as amount evolved O_2(g) in µmol / bulk amount cobalt in µmol. Turnover frequency (TOF) is calculated as TN / time in seconds from the initial slope of the kinetic curve.

Results and discussion

Crystal structures

$Co_4(SeO_3)_3Cl_2$. Blue single crystals of compound **1** were synthesized via solid state reactions by heating at 550°C for 96 h. It crystallizes in the orthorhombic system, space group *Pnma*. The crystal structure is an open framework having cavities along [100], see Figure 1a. There are two crystallographically different Co-atoms, both showing distorted octahedral coordination. Co(1) has distorted octahedral $[Co(1)O_4Cl_2]$ coordination where the oxygen atoms are in the basal square plane. The Co-O distance varies in the range 2.024(2) – 2.373(2) Å and the Co-Cl distances are 2.401(1) and 2.704(1) Å. Co(2) has distorted octahedral $[Co(2)O_5Cl]$ coordination with Co-O distances in the range 2.024(2) – 2.187(2) Å and the Co-Cl distance is 2.431(1) Å. The Co(1) octahedra connect by corner sharing via Cl(1) to form chains along [100]. The Co(2) octahedra form dimers via edge sharing at two common O(4). The dimers are connected to the Co(1)-chains by corner and edge sharing to form layers parallel with the (101) plane. The layers are further connected by corner sharing via O(3) in the $[Co(1)O_4Cl_2]$ polyhedra to build up the three dimensional structure. There are two crystallographically unique Se atoms both having $[SeO_3]$ coordination with Se – O bond distances in the range 1.622(2) – 1.731(2) Å; the stereochemically active lone-electron pair, E on the Se^{4+} ions, complete distorted $[SeO_3E]$ tetrahedra. All oxygen atoms are shared in between both Co-octahedra and SeO_3 groups. The SeO_3E polyhedra do not polymerise in the structure and are connected to the Co-oxochloride network by corner and edge sharing so that the lone pairs on Se point into the channels of non-bonding volume in the crystal structure. The channels have a shortest diameter in between O1 – O1 that is ~4.6 Å. If we assume a Se – E efficient distance of 1.22 Å according to Galy [15] then the channel diameter reduces to ~2.9 Å. Bond Valence Sum (BVS) calculations support the oxidation state for the ingoing atoms as suggested from the structure solution; Co^{2+}, Se^{4+}, O^{2-}, Cl^-, see Supporting material. The Cl atom is slightly underbonded and gets a BVS value of 0.82 vu. However, it is very common with underbonded halide ions in this family of oxohalides and the present relatively high value is to be regarded as a strong indication that Cl is a part of the covalent network rather than being mainly a counter ion.

Specific surface areas (S_{BET}) were calculated from the N_2 adsorption measurements using standard expressions for Brunauer–Emmet–Teller (BET) isotherms and gave a total pore volume of 0.00430 cm^3/g and a BET surface area of 1.94 m^2/g for compound **1**. The small surface area shows that it is likely that the pores are not accessible even for H_2O molecules and that the water oxidation reaction can take place only at the particle surfaces, as suggested already by the small diameter of the channels.

$Co_3Se_4O_{10}Cl_2$. Compound **2** was prepared at the same temperature as compound **1**. It crystallizes in the monoclinic system, space group *C2/m*. Chains of $[Co_3O_8Cl_2]_\infty$ extend along [001] and are connected by $[Se_2O_5]$ groups. This crystal structure also comprises channels formed due to presence of the terminating species selenium lone-pairs and chlorine anions and run along [100] and [001], see Figure 1b. There is one crystallographically unique Se atom having the oxidation state +4 as suggested by bond valence sum calculations (BVS). The Se atom is bonded to three O at distances in the range 1.657(6) – 1.776(3) Å to form the typical $[SeO_3]$ trigonal pyramid where the stereochemically active lone electron pair complete a distorted tetrahedron. The $[SeO_3]$ polyhedra connect via O(3) to form $[Se_2O_5]$ groups. It is rare that $[SeO_3]$ polyhedra polymerizes while it is more common for $[TeO_3]$ polyhedra [16]. Some examples of other compounds containing $[Se_2O_5]$ groups are $A_2(Se_2O_5)_3$ ($A = Al^{3+}$, Ga^{3+} or In^{3+}) [17], and $B_4(VO_2)_2(SeO_3)_4(Se_2O_5)$ ($B = Sr^{2+}$ or Pb^{2+}) [18]. There are two crystallographically different Co^{2+} ions which both have octahedral $[CoO_4Cl_2]$ coordination, however, they are not identical. In $[Co(1)O_4Cl_2]$ the Cl atoms are *trans* to each other and the O atoms form a square plane. In $[Co(2)O_4Cl_2]$ the Cl atoms are *cis* to each other. The Co – O distances vary in the range 2.060(5) to 2.116(5) Å and the Co – Cl distances vary in the range 2.424(2) – 2.520(19) Å. The $[Co(1)O_4Cl_2]$ and $[Co(2)O_4Cl_2]$ octahedra are connected via edge sharing to form $[Co_3O_8Cl_2]_\infty$ chains running along [001], see Figure 1b. The Cl^- anion has a coordination number of three which is unusually high for compounds in the M-L-O-X system, where M is a transition metal cation, L = p-block lone pair element such as Se^{4+}, Te^{4+}, or Sb^{3+}, X = halide anion. Most other such compounds have a coordination number for Cl of only one or two [2-3]. However, BVS calculations give a value as low as 0.83 for Cl indicating that it is still underbonded despite the high coordination number. The diameter of the channels (~3.2 Å) is decided by the O3 – O3 distance. The shortest estimated distance between two lone-pairs over the channel is ~4.3 Å.

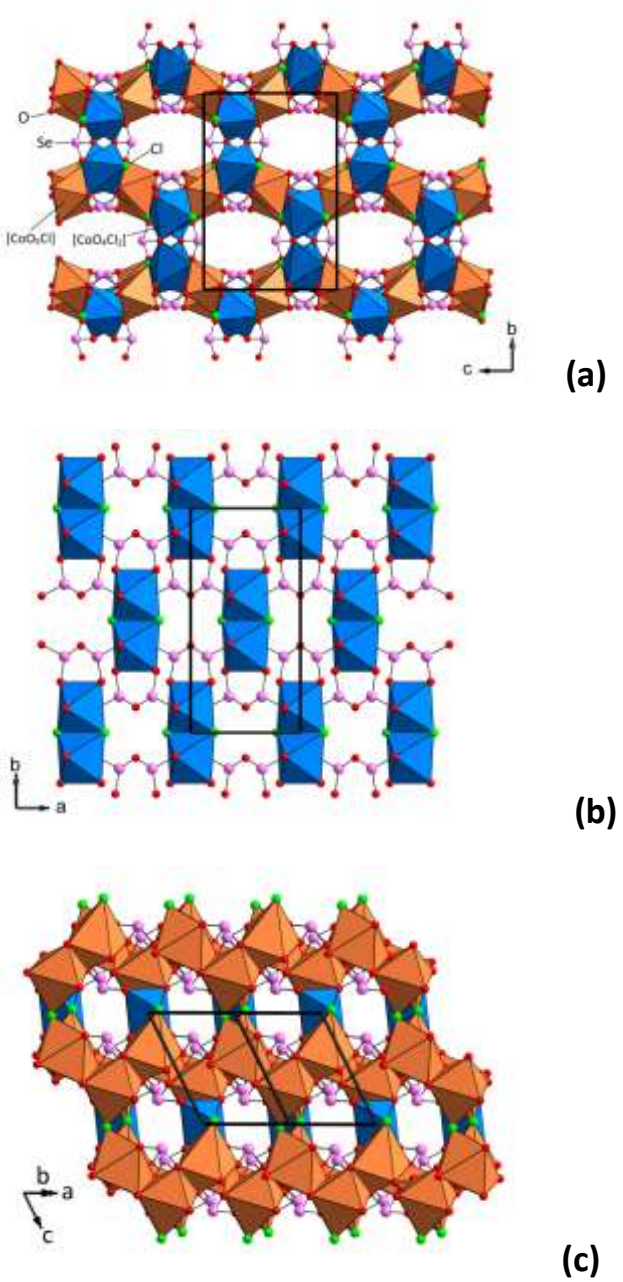

Figure 1 Overview of the crystal structures. **a,** $Co_4Se_3O_9Cl_2$, **1**, along [100]. **b,** $Co_3Se_4O_{10}Cl_2$, **2**, edge sharing $[CoO_4Cl_2]$ octahedra extend along [001] to form $[Co_3O_8Cl_2]_\infty$ chains. The chains are connected by $[Se_2O_5]$ groups to form the 3D framework. **c,** $Co_5Se_4O_{12}Cl_2$, **3**, along [-110]. The same colour coding for atoms and polyhedra are used in the different structure drawings.

$Co_5Se_4O_{12}Cl_2$. Purple single crystals of **3** crystallize in the triclinic space group *P-1* and is to the best of our knowledge the only compound previously described in the system Co^{2+}-Se^{4+}-O-Cl [1], however, it has not been tested before as a catalyst for water oxidation. Like in compound **1** the cobalt atoms in **3** have $[CoO_5Cl]$ and $[CoO_4Cl_2]$ coordination's and the selenium forms $[SeO_3]$ polyhedra that do not polymerise. The crystal structure displays channels along [-110], see Figure 1c. Here the Cl1 – Cl1 distance gives rise to the smallest diameter of the channels (~4.1 Å). The closest distance in between two lone-pairs over the channel is ~4.4 Å.

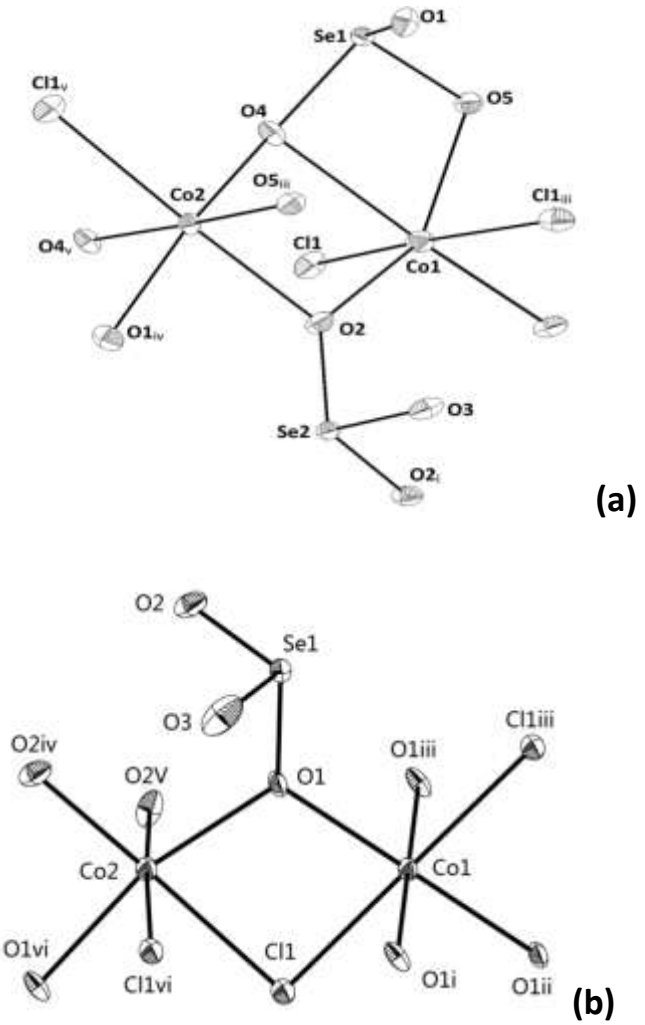

Figure 2 (a) A displacement ellipsoid diagram of $Co_4(SeO_3)_3Cl_2$ **(1)** showing the coordination around the cations. Atomic displacement parameters are given at the 50% probability level. Symmetry codes: (i) x, 0.5-y, z; (ii) 0.5+x, y, 0.5-z; (iii) -0.5+x, y, 0.5-z; (iv) 0.5-x, 1-y, -0.5+z; (v) 1-x, 1-y, -z]. **(b)** The asymmetric unit plus selected equivalents to show the coordination around the cations in **(2)** $Co_3Se_4Cl_2O_{10}$. Symmetry codes: (i) 1-x, y, 1-z ; (ii) 1-x, y, -z; (iii) x, y, -1+z; (iv) 1-x, 1-y, 1-z; (v) x, 1- y, -1+z; (vi) 0.5-x, 0.5+y, 1-z; (vii) -x, 1-y, -z; (viii) 0.5+x, 0.5+y, z; (ix) x, 1- y.

Water oxidation

The activity of the three different cobalt oxohalides as water oxidation catalysts was compared with CoO and $CoCl_2$ by suspending them in a phosphate buffer at pH 6.0 and adding the homogeneous oxidant $Ru^{3+}(bpy)_3(PF_6)_3$. Immediate evolution of oxygen then ensued and ceased only when the oxidant was depleted. The ranking of the catalysts is shown in Figure 3 and the trend is that the cobalt oxohalides show higher catalytic activity than $CoCl_2$, but are less active than CoO. In order to ensure that the evolved oxygen was derived from oxidation of water, oxidation experiments were also performed in ^{18}O labeled water. The isotope ratios in the

evolved oxygen indicate that at least 90% of the oxygen originated from water. From the simplified perspective that a cobalt atom in the oxo-halides binds to chloride- as well as oxide ions, see Figure 2, the catalytic activity should correspondingly be in between CoO and $CoCl_2$. Given also that $Co_3(PO_4)_2$ has a low solubility product, $K_{sp} \approx 10^{-44}$, the 0.1 M phosphate buffer environment at pH 6.0 will likely cause $CoCl_2$ to form $Co_3(PO_4)_2$ during dissolution while CoO is not destroyed by reacting with the phosphate buffer. This simple model can further be applied on the oxohalide compounds assuming that the Cl atoms are easier to dissociate leaving cobalt to interact with PO_4^{3-}, possibly resulting in rapid formation of a Co-O-PO_4 arrangement at the surface.

Interestingly, the reaction kinetics for CoO is initially slower than for the oxohalides but the total yield of oxygen is much higher, see Figure 3. If pure CoO is the ideal catalyst the activity would also be accordingly fast. It therefore seem possible that the phosphate ion actually is a co-actor in catalysis but it needs longer time to form new bonds leading to a Co-O-PO_4 arrangement at the surface of CoO particles in comparison to the oxohalides that have Co-Cl bonds that are more reactive than Co-O bonds and thus more easily can be replaced by Co-PO_4 bonds. However, the fast initial kinetics of the oxohalides slow down with time, possibly by the presence of chlorine ions that in an oxidative environment can produce Cl_2(g), ClO_2^- or ClO_3^- species that destructively react with the bpy ligand of the $Ru(bpy)_3^{3+}$ oxidant resulting in a lower total yield of oxygen than CoO.

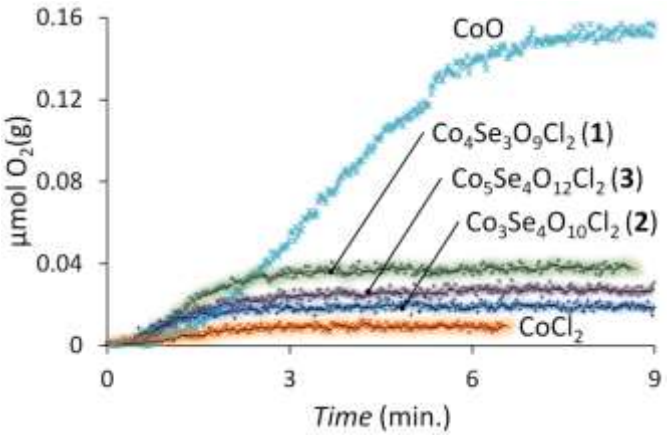

Figure 3 Evolution of oxygen from water oxidation using $Ru^{3+}(bpy)_3(PF_6)_3$ as oxidant and the three cobalt oxohalides in comparison with CoO and $CoCl_2$. The molar ratios were kept comparable: ~2.0 µmol oxidant and ~1.7 µmol Co per catalyst.

During the catalytic process cobalt changes between 3+ and 4+ oxidation states, the flexible electron configurations of cobalt throughout the different oxidation stages with unpaired electrons occupying the e_g-orbitals are highly depending on the ligand field [19]. Hence, we suggest that a Co-O-PO_4 arrangement of a certain proportion is favorable for the cobalt electron configurations and acts as the active species in catalysis. Several studies have proposed a cobalt oxo-cubane arrangement of edge sharing cobalt octahedra to efficiently catalyze water oxidation [19-23]. None of compounds **1-3** exhibit a strict cobalt oxo-cubane in their pristine structure since the cobalt octahedra contain both O and Cl. However, it is shown that compound (**1**) is active also upon a second addition of $Ru(bpy)_3^{3+}$, see Figure 4, indicating the stability of the active species in the highly oxidative environment.

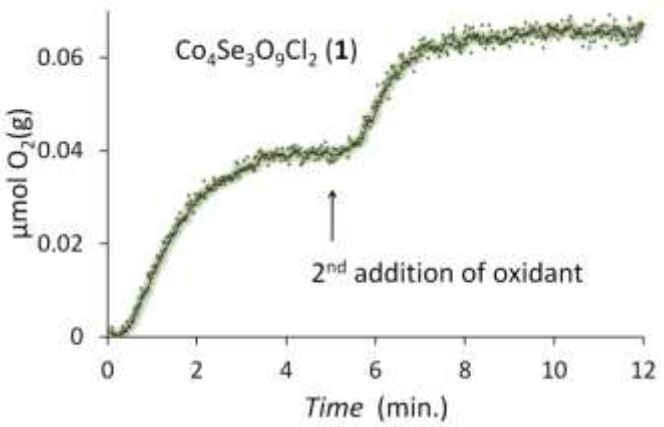

Figure 4 Evolution of oxygen from water oxidation after two separate additions of the oxidant (~2.1 µmol each) using compound (**1**) as catalyst (13.2 µmol Co).

A question is whether the proposed active Co-O-PO_4 arrangement is located (i) on the surface of a solid (ii) as a suspended nano-sized solid or (iii) as a dissolved complex. This question also sheds light on the problem of relating TN (and TOF) to the true amount of active catalytic sites; currently we use the bulk amount of cobalt in the catalyst for comparison. This is a large underestimation as the majority of cobalt atoms are isolated from catalysis as the crystal bulk is not exposed to participate in the WOC.

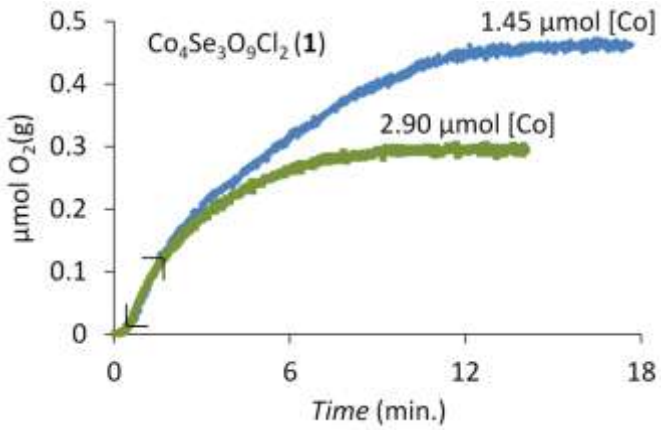

Figure 5 Same addition of oxidant (5.6 µmol) to two different addition levels of compound **(1)** (1.45µmol and 2.90 µmol Co). The lower addition of compound (**1**) yields more oxygen than the higher addition. This can be explained by that compound (**1**) also catalyze decomposition of the oxidant in a way that does not yield oxygen.

The experimental set-ups have shown to be critical; the studies get complicated by that *e.g.* compound (**1**) also seem to catalyze a decomposition of the oxidant in a process that does not yield evolution of O_2(g); the amount of evolved oxygen is less at a higher ratio of catalyst to oxidant, see Figure 5. The turnover numbers increase proportionally to the amount of oxidant used. The oxygen yield for various amounts of $Ru(bpy)_3^{3+}$ at a constant amount of catalyst with corresponding turnover numbers is shown in Figure 6. Upon higher additions of oxidant the initial slope of the kinetic curve increases, which indicates a higher reaction order than zero. We chose the experiment with the highest TN 1.0 for calculating the TOF from the initial kinetic data then TOF = $5.4 \cdot 10^{-3}$ s^{-1} per Co atom. Higher additions of $Ru(bpy)_3^{3+}$ allow for greater evolution of

oxygen, however, the small difference in catalytic performance for oxygen evolution of the oxohalides and $CoCl_2$ will then be masked by the higher oxygen yield for all catalysts. By empirically adjusting the amounts between the catalyst and the oxidant a suitable ratio appears for studying their catalytic properties. The color changes from light green Ru^{3+}-complex to a bright orange Ru^{2+}-complex during analysis and this is an important indicator on how side reactions are evolving in relation to the oxygen evolution. Experiments with only $Ru^{3+}(bpy)_3(PF_6)_3$ in phosphate buffer showed insignificant decay during 30 min. However, earlier studies of $Ru^{3+}(bpy)_3(PF_6)_3$ in phosphate buffer at pH 7.2 show that the oxidant is spontaneously decomposed within ca 30min and that surprisingly no oxygen is generated [24]. Yin *et al.* [25] have earlier introduced addition of bipyridine to bind free cobalt ions to quench their activity in water oxidation. However, in our experiments an instant color change from green to orange occurred without any gas evolution, suggesting that this experiment is not suitable for the heterogeneous catalysts in this study.

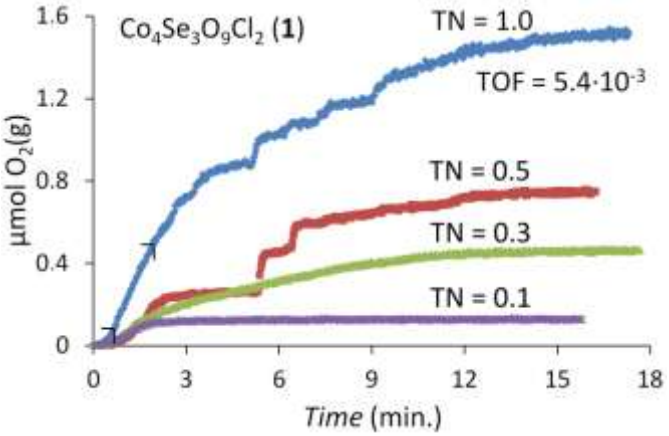

Figure 6 Evolution of oxygen from water oxidation using different amounts of oxidant [22.4 µmol (blue), 11.21 µmol (red), 5.6 µmol (green) and 2.0 µmol (lilac)] and a fixed amount of compound (**1**) as catalyst (1.45 µmol bulk Co) yielding different turnover numbers (TN). The irregular shapes of the two upper curves originate from bursting oxygen bubbles during analysis because of the relatively large amounts of oxidant used. Line breakers indicate the initial kinetic data points used for TOF calculation ($R^2 = 0.998$).

The maximum theoretical yield of the measured oxygen is given according to $4Ru^{3+} + 2H_20 \rightarrow 4Ru^{2+} + 4H^+ + O_2$. In our experiments the practical yield is around 25%, leaving the question of why the water oxidation reaction cannot utilize the total initial amount of $Ru(bpy)_3^{3+}$ and why does this differ between catalysts? The presence of Cl^- has been discussed above, however, in the oxidative environment caused by the high potential of Ru^{3+} other oxidative side reaction of organic ligands is probably a major pathway. If such oxidation reaches C^{4+} then evolved CO_2 will be detected in the mass spectrometer, although none of the experiments in this study have evolved significant amounts of CO_2 and hence any oxidation of carbon must have reached a lower oxidation state. Further, it is also possible that water will not be fully oxidized but cause H_2O_2 as an intermediate that is unstable at pH = 6.0 and that may cause a delay in reaching equilibrium so that O_2 will be released at a slower rate. Both these side reactions may vary with the efficiency of the catalyst; potentially a catalyst may work better for catalyzing the side reactions better than the desired water oxidation. The yield has been around 25% independent of the amount of ruthenium used, see Figure 6, which indicates that it is the catalyst, rather than the accessibility of oxidant, that regulates the side reactions as is also supported by the measurements shown in Figure 5. A possible side reaction is a one-on-one electron redox reaction simplified as $Co^{2+} + Ru^{3+} \rightarrow Co^{3+} + Ru^{2+}$ contributing to the depletion of Ru^{3+}.

Conclusions

Two new oxohalides $Co_4Se_3O_9Cl_2$ and $Co_3Se_4O_{10}Cl_2$ have been synthesized by solid state reactions. $Co_4Se_3O_9Cl_2$ crystallizes in the orthorhombic space group *Pnma* The crystal structure is made up of $[CoO_4Cl_2]$, $[CoO_5Cl]$ and $[SeO_3]$ polyhedra and show cavities along [100]. The shortest diameter in between two oxygen atoms over such a channel is ≈4.6 Å. However, the stereochemically active lone-pairs on Se occupy space in the cavities and therefore the BET surface area was found to be only 1.9 m^2/g. The compound $Co_3Se_4O_{10}Cl_2$ crystallizes in the monoclinic space group *C2/m* and is made up of $[CoO_4Cl_2]$ and $[SeO_3]$ polyhedra. The Se-polyhedra polymerize to $[Se_2O_5]$ groups.

The two new oxohalides were tested as water oxidation catalysts and compared with the previously found oxohalide $Co_5Se_4O_{12}Cl_2$ and also with CoO and $CoCl_2$. The one electron oxidant $Ru(bpy)_3^{3+}$ was used as oxidant in a phosphate buffer and it was found that the activity of the oxohalide species were in between CoO and $CoCl_2$. The water oxidation reaction experiments resulted in a discussion around the catalytic activity, side reactions and finally in a suggestion that the active catalytic specie is a Co-O-PO_4 arrangement with variable number of O and PO_4 groups up to an octahedral arrangement. The study also highlights the difficulties of comparing different heterogeneous catalysts. This indicates the need for continuous investigation of the different mechanisms involved in aqueous-heterogeneous catalysis.

Acknowledgements

The Swedish Research Council, the Swedish Energy Agency and the Knut and Alice Wallenberg Foundation are acknowledged for financial support.

Notes and references

[a] Department of Materials and Environmental Chemistry, Stockholm University, SE-106 91 Stockholm, Sweden.
[b] Permanent address: Department of Chemistry, University of Engineering and Technology, Lahore - 54890, Pakistan.
[c] Department of Organic Chemistry, Stockholm University, SE-106 91 Stockholm, Sweden.

† Further details on the crystal structural investigations can be obtained from the Fachinformationszentrum Karlsruhe, Abt. PROKA, 76344 Eggenstein-Leopoldshafen, Germany (fax +49-7247-808-666; E-mail: crysdata@fiz-karlsruhe.de) on quoting the depository number CSD-425434 for **(1)** $Co_4Se_3O_9Cl_2$ and CSD-425433 for **(2)** $Co_3Se_4O_{10}Cl_2$.

Electronic Supplementary Information (ESI) available: [Atomic coordinates and equivalent isotropic displacement parameters, selected bond lengths (Å) and angles (°), results from bond valence sum (BVS) calculations]. See DOI: 10.1039/b000000x/

1 R. Becker, M. Prester, H. Berger, P.H. Lin, M. Johnsson, D. Drobac and I. Zivkovic, *J. Solid State Chem., 2007*, **180**, 1051.
2 D. Zhang, M. Johnsson, H. Berger, R.K. Kremer, D. Wulferding and P. Lemmens, *Inorg. Chem.*, 2009, **48**, 6599.

3 M. Johnsson, K.W. Törnroos, P. Lemmens and P. Millet, *Chem. Mater.*, 2003, **15**, 68.
4 V. Shafirovich, N.K. Khannanov and V.V Strelets, *Nov. J. Chim.*, 1980, **4**, 81.
5 G.L. Elizarova, L.G. Matvienko, N.V. Lotzkina, N.V. Parmon and K.I. Zamarev, *React. Kinet. Catal. Lett.* 1981, **16**, 191.
6 B.S. Brunschwig, M.H. Chou, C. Creutz, P., Ghosh and N.A. Sutin, *J. Am. Chem. Soc.*, 1983, **105**, 4832.
7 M.W. Kanan and D.G. Nocera, *Science, 2*008, **321**, 1072.
8 Oxford diffraction, CrysAlisCCD and CrysAlisRED. Oxford Diffraction Ltd., Abingdon, Oxfordshire, England (2006).
9 G.M. Sheldrick, *Acta Cryst. A64*, 112-122 (2008).
10 G. Bergerhoff, 1996, DIAMOND, Bonn, Germany.
11 I.D. Brown and D. Altermatt, *Acta Cryst.*, 1985, **B41**, 244.
12 Y. Gao, T. Åkermark, J.H. Liu, L.C. Sun and B. Åkermark, *J. Am. Chem. Soc.*, 2009, **131**, 8726.
13 Y. Xu, T. Åkermark, V. Gyollai, D. Zou, L. Eriksson, L. Duan, R. Zhang, B. Åkermark and L. Sun, *Inor. Chem.*, 2009, **48**, 2717.
14 R.E. DeSimone and R.S. Drago, *J. Am. Chem. Soc.*, 1970, **92**, 2343.
15 J. Galy, G. Meunier, S. Andersson and E. Åström, *J. Solid State Chem.*, 1975, **13**, 142.
16 J.-G. Mao, H.-L. Jiang and F. Kong, *Inorg. Chem.*, 2008, **47**, 8498.
17 K.M. Ok and P.S. Halasyamani, *Chem. Mater.*, 2002, **14**, 2360.
18 J. Yeon, S.-H. Kim, S.D. Nguyen, H. Lee and P.S. Halasyamani, *Inorg. Chem.*, 2012, **51**, 609.
19 U. Maitra, B.S. Naidu, A. Govindaraj and C.N.R. Rao, *Proc. Nat. Academ. Sci.*, 2013, **110**, 11704.
20 J. Rosen, S. Gregory and F. Jiao, *J. Am. Chem. Soc.*, 2013, **135**, 4516.
21 M.D. Symes, D.A. Lutterman, T.S. Teets, B.I. Anderson, J.J. Breen and D.G. Nocera, *Chem. Sus. Chem.*, 2013, **6**, 65.
22 N.S. McCool, D.M. Robinson, J.E. Sheats and G.C. Dismukes, *J. Am. Chem. Soc.*, 2011, **133**, 11446.
23 E.Y. Tsui, R. Tran, J. Yano and T. Agapie, *Nat. Chem*. 2013, **5**, 293.
24 E.A. Karlsson, B.-L. Lee, T. Åkermark, E.V. Johnson, M.D. Kärkäs, Ö. Hansson, J.-E. Bäckvall and B. Åkermark, *Angew. Chem. Int Ed., 2011*, **50**, 11715.
25 Q. Yin, C. Besson, Y.V. Geletii, D.G. Musaev, A.E. Kutznetsov, Z. Luo, K.I. Hardcastle and C.L. Hill, Science, 2010, **328**, 342.